Comparison of standard OFDM/BFDM to bandwidth-efficient pulse shape optimized MC schemes

Peter Jung, Gerhard Wunder and Holger Boche
Heinrich-Hertz-Institute for Communication Technology
Department of Broadband Mobile Communication Networks
{jung,wunder,boche}@hhi.de

***Abstract*— Multicarrier transmission schemes are promising candidates for next generation broadband wireless communication systems. Many optimizations for time–variant channels of this transmission scheme supported by results from time–frequency analysis were proposed, so that a generalized characterization of several system performance aspects is mandatory. Here we give a joint formulation of the frequency offset as the most basic time–variant distortion in mobile channels as well we discuss pulse design aspects.**

***Index Terms*— Multicarrier transmission, OFDM, BFDM, NOFDM, frames, Gabor theory, Biorthogonal**

I. Introduction

Due to the increased symbol length conventional multicarrier (MC) transmission over frequency subcarriers benefits in multipath channels from the lower time dispersion per subcarriers. That results in a reduced amount of intersymbol interference compared to a single carrier system operating at the same data rate. Obviously this choice of the carriers matches the time–invariant channel. The most popular MC setup in this domain – orthogonal frequency-division multiplexing (OFDM) – has already been implemented into several standards such as DAB and DVB-T.

Understanding the time–varying channel as statistically time and frequency shifts gives rise to the question what are then the approximate invariant directions corresponding to the subcarriers in OFDM. The mean power profile of these shifts creates a partition of the *time–frequency–plane* (TF–plane) into uncorrelated regions and it is intuitivly clear that the optimal time–frequency–carriers bearing the information have to match this profile. Such an adaption to the channel requires control over the transmitter and receiver pulse parameters – especially their localization – which is not possible with the conventional OFDM scheme. Having this picture in mind and additionally motivated by the reduced spectral efficiency of OFDM due to the cyclic prefix (from now on cp–OFDM) new MC transmission techniques have been proposed by several authors. Most of the contributions in this field are inspired by time-frequency analysis and Gabor theory [1] that gives the mathematical description for compositions of modulations and time shifts of a single function.

Here we give a joint description of the most basic time variant distortion – the frequency offset – which covers the more general framework of biorthogonal frequency-division multiplexing (BFDM) [2], [3] and the approach of "Bandwidth Efficient Nonorthogonal Multicarrier Transmission" (NOFDM) established in [4]. The motivation behind this is the effect of carrier frequency mismatching as well the first steps towards exploring time-variant channels. In addition we show that careful pulse shaping significantly improves the performance of the BFDM/NOFDM approaches.

II. System Description

A. Generalized multicarrier model

Let $\{\gamma_{mn}\} \subset \mathcal{L}^2(\mathbb{R})$ (the square–integrable complex–valued functions on $\mathbb{R}$) with $(mn) \in \mathcal{I}$ where $\mathcal{I}$ is a (doubly) countable index set. MC signaling modulates $x_{mn} \in \mathbb{C}$ onto $\{\gamma_{mn}\}$ so that the baseband transmit signal can be written as

$$s(t) = \sum_{(mn)\in\mathcal{I}} x_{mn}\gamma_{mn}(t) = \mathbf{\Gamma}(t)\boldsymbol{x} \tag{1}$$

with the notation $\boldsymbol{x} = (\ldots, x_{mn}, \ldots)$ and $\mathbf{\Gamma}(t) = (\ldots, \gamma_{mn}(t), \ldots)^T$. The received signal is

$$r(t) = (\boldsymbol{\mathcal{H}}\mathbf{\Gamma})(t)\boldsymbol{x} + n(t) \tag{2}$$

where $\boldsymbol{\mathcal{H}}$ denotes the linear channel and $n(t)$ the AWGN noise. A linear MC receiver projects the received signal onto a set of receiver functions $\{g_{mn}\} \subset \mathcal{L}^2(\mathbb{R})$.

$$\begin{aligned}\tilde{\boldsymbol{x}} &:= \mathbf{C}\int \boldsymbol{G}^*(t)[(\boldsymbol{\mathcal{H}}\mathbf{\Gamma})(t)\boldsymbol{x} + n(t)]dt \\ &= \mathbf{C}\underbrace{[\int \boldsymbol{G}^*(t)(\boldsymbol{\mathcal{H}}\mathbf{\Gamma})(t)dt]}_{H}\boldsymbol{x} + \underbrace{\mathbf{C}\int \boldsymbol{G}^*(t)n(t)dt}_{\tilde{\boldsymbol{n}}}\end{aligned} \tag{3}$$

and obtains the received symbols $\tilde{\boldsymbol{x}} = \mathbf{C}H\boldsymbol{x} + \tilde{\boldsymbol{n}}$ where again $\boldsymbol{G}(t) = (\dots, g_{mn}(t), \dots)^T$ ($\cdot^*$ means conjugate transpose in the remaining indices/variables). The linear map $\mathbf{C}$ serves as an equalization of the channel and $\tilde{\boldsymbol{n}}$ is the projected noise with power $\sigma^2_{\tilde{n}}$. $H = (H_{kl,mn})$ describes the coupling of the subcarriers in terms of the transmitter and receiver carrier functions

$$H_{kl,mn} = g^*_{kl}\boldsymbol{\mathcal{H}}\gamma_{mn} = \int \bar{g}_{kl}(t)(\boldsymbol{\mathcal{H}}\gamma_{mn})(t)dt \qquad (4)$$

In the absence of channel and noise biorthogonality $g^*_{kl}\gamma_{mn} = \delta_{km}\delta_{ln}$ ensures perfect linear reconstruction of arbitrary $\boldsymbol{x}$'s and implies linear independency of $\{\gamma_{mn}\}$ and $\{g_{mn}\}$. To make use of simpler algebra we define the action of the adjoint of $\boldsymbol{G}$ as

$$(\dots, g^*_{mn}f, \dots) = \boldsymbol{G}^* f = \int \boldsymbol{G}^*(t)f(t)dt \qquad (5)$$

$\boldsymbol{G}^*$ is often called the analyse operator where $\boldsymbol{\Gamma}$ is the synthese operator. Biorthogonality writes then $\boldsymbol{G}^*\boldsymbol{\Gamma} = \mathbb{I}_{\mathcal{I}}$ (the identity on $\mathcal{I}$). If then $\{\gamma_{mn}\}$ or $\{\overline{g_{mn}}\}$ are approximate eigenfunctions of $\boldsymbol{\mathcal{H}}$

$$\mathbf{C}H = \mathbf{C} \cdot \boldsymbol{G}^*\boldsymbol{\mathcal{H}}\boldsymbol{\Gamma} \approx \mathbf{C} \cdot \text{diag}\{\dots, h_{mn}, \dots\} \overbrace{\boldsymbol{G}^*\boldsymbol{\Gamma}}^{\mathbb{I}_{\mathcal{I}}} \qquad (6)$$

with the eigenvalues h_{mn} simple channel equalization with $\mathbf{C} = \text{diag}\{\dots, h^{-1}_{mn}, \dots\}$ is possible. From this point of view it is clear that cp–OFDM with exponential transmitter and receiver carrier functions is "optimal" for time–invariant channels, where for time–variant szenarios one can do better. For the more general MC concept we choose γ_{mn} as time–shifted and modulated versions of a single prototype γ. Further the time shifts $\mathcal{T}_\alpha$ and modulations $\mathcal{M}_\beta$. should be from the regular lattice $(\alpha, \beta) \in T\mathbb{Z} \times F\mathbb{Z}$, thus

$$\gamma_{mn}(t) = (\,\mathcal{M}_{mF}\mathcal{T}_{nT}\,\gamma\,)(t) = \gamma(t - nT)e^{i2\pi mFt} \qquad (7)$$

where TF denotes the volume of the TF–sampling cell of the time–frequency plane. These *Gabor sets* exhibit nice structural properties. We refere here to the rich literature on Gabor theory [1]. For short notation - one of them is the balance between completeness in $\mathcal{L}^2(\mathbb{R})$ and linear independency. For $TF \leq 1$ the Gabor set could [1] be complete and establish a *frame* (critical sampling or oversampling of the TF-plane), where for $TF > 1$ it is incomplete (undersampling of the TF-plane).

The volume TF is directly related to the spectral efficiency $\epsilon = \frac{1}{TF}$ of the MC–signaling[2]. With the normalization $\|\gamma\|^2 = TF$ the transmit power is independent of ϵ. For cp–OFDM with a cyclic prefix of the length $T_{cp} \geq 0$ the width of the rectangular transmitter and receiver pulse is $T - T_{cp}$. The spacing of the carriers is therefore coarser, hence $F = (T - T_{cp})^{-1}$ and $\epsilon \leq 1$. For $T_{cp} = 0$ it's a critical sampling of the TF–plane ($TF = 1$). As long the strict Gabor scheme is used at critical sampling the *Balian-Low-Theorem* [5] states that either in time or in frequency the pulses will have bad localization properties.

Therefore concentrating first on $TF > 1$ we end up with the BFDM-like transmission model. $\boldsymbol{G}^*$ can be computed for a given $\boldsymbol{\Gamma}$ as its left inverse $\boldsymbol{G}^* = (\boldsymbol{\Gamma}^*\boldsymbol{\Gamma})^{-1}\boldsymbol{\Gamma}^*$. $\boldsymbol{G}$ then exhibits again the Gabor structure. For the projected noise follows in general $\mathbf{E}\{\tilde{\boldsymbol{n}}\tilde{\boldsymbol{n}}^*\} \neq \sigma^2_n\mathbb{I}_{\mathcal{I}}$.

Most of the work on Gabor MC schemes were based on the assumption of linear independency. The question is how we could overload the bandwidth in an optimal way and increase ϵ. Inspired from the work in [6] we extent their approach in a more compact formulation.
If the $\{\gamma_{mn}\}$ form a frame for the closed subspace $\mathcal{B} \subset \mathcal{L}^2(\mathbb{R})$ of the possible signals, that is

$$0 < A \leq \boldsymbol{\Gamma}\boldsymbol{\Gamma}^* \leq B < \infty \qquad (8)$$

then there exists dual frames $\{g_{mn}\}$[3] with $\boldsymbol{\Gamma}\boldsymbol{G}^* = \mathbb{I}_{\mathcal{B}}$. The ordering relations are in respect to the operator norms on $\mathcal{B}$. The canonical choice among all possible dual frames is the right inverse of $\boldsymbol{\Gamma}$ given as $\boldsymbol{G}^* = \boldsymbol{\Gamma}^*(\boldsymbol{\Gamma}\boldsymbol{\Gamma}^*)^{-1}$ having the minimal energy. A correlation based receiver which has channel knowlegde would project the $r(t)$ on the channel–distorted transmit carrier functions, that is an application of $(\boldsymbol{\mathcal{H}}\boldsymbol{\Gamma})^*$ on $r(t)$. Practical implementations could rely here again on efficient DFT–filterbanks if the channel is fixed. If not it is properly easier to do the channel equalization again with $\mathbf{C}$ instead of adapting the filterbank, hence

$$(\boldsymbol{\mathcal{H}}\boldsymbol{\Gamma})^* = (\boldsymbol{\mathcal{H}}\boldsymbol{\Gamma})^* \overbrace{\boldsymbol{\Gamma}\boldsymbol{G}^*}^{\mathbb{I}_{\mathcal{B}}} = (\overbrace{\boldsymbol{\Gamma}^*\boldsymbol{\mathcal{H}}\boldsymbol{\Gamma}}^{\mathbf{C}})^*\boldsymbol{G}^* = \mathbf{C}^*\boldsymbol{G}^* \qquad (9)$$

where $\mathbf{C}$ is the channel action in terms of the transmit functions only. Note here that this differs only in $\mathbf{C}$ from the BFDM transmission model. The input to the symbol estimation is $\boldsymbol{u} = \mathbf{C}^*\boldsymbol{G}^*r(t)$ and the symbol estimation itself is the following equation

$$\boldsymbol{u} = \overbrace{(\boldsymbol{\mathcal{H}}\boldsymbol{\Gamma})^*(\boldsymbol{\mathcal{H}}\boldsymbol{\Gamma})}^{A}\boldsymbol{x} + \overbrace{(\boldsymbol{\mathcal{H}}\boldsymbol{\Gamma})^*n(t)}^{\tilde{\boldsymbol{n}}} = A\boldsymbol{x} + \tilde{\boldsymbol{n}} \qquad (10)$$

where the singular A could rewritten as $A = \mathbf{C}^*\boldsymbol{G}^*\boldsymbol{G}\mathbf{C}$. A suboptimal solution of Equ.(10) on a discrete alpha-

[1] still depending on $\gamma(\cdot)$

[2] In general is $\epsilon = \frac{\eta}{TF}$ where η is the number of bits per symbol. In the following we set here $\eta = 1$.

[3] the dual frames have again Gabor structure

bet is accomplished iterative using the Gauss–Seidel algorithm with serial hard decisions, instead of a full-complexity likelihood maximization (details see [6]). For our simulations serial hard decisions start after 9 linear cycles. The maximal number of iterations was limited to 30 and the stop precisison $\epsilon = 10^{-11}$.

B. Unitary channel

Considering now due to sampling with respect to ϵ and windowing $\mathcal{I} = \{(mn) | m = 0 \dots M-1, n = 0 \dots N-1\}$ where M denotes the number of modulations and N the number of time shifts. It can be shown that Equ.(8) still holds in a periodized model [7], [8]. Expressing for independently zero mean distributed x_{mn} the energy of the carrier (kl) as

$$\begin{aligned} 0 \leq \mathbf{E}\{|\tilde{x}_{kl}|^2\} &= \sum_{(mn)\in\mathcal{I}} |H_{kl,mn}|^2 \overbrace{\mathbf{E}\{|x_{mn}|^2\}}^{=1} \\ &= g_{kl}^* \boldsymbol{\mathcal{H}} \boldsymbol{\Gamma}\boldsymbol{\Gamma}^* \boldsymbol{\mathcal{H}}^* g_{kl} \leq B \|\boldsymbol{\mathcal{H}}^* g_{kl}\|^2 = B\|g\|^2 \end{aligned} \tag{11}$$

with the last step only for unitary $\boldsymbol{\mathcal{H}}$. For $\{\gamma_{mn}\}$ being a frame there is in addition

$$0 < A\|g\|^2 \leq \mathbf{E}\{|\tilde{x}_{kl}|^2\} \leq B\|g\|^2 \tag{12}$$

the lower frame bound A. In the case of a tight frame we have $A = B$ stating the energy conservation. Splitting up the energy in the carrier (kl) into a attentuated "correct" signal energy[4] $|s|^2$ and an interfering term I_{ext} from $(mn) \neq (kl)$ yields

$$\begin{aligned} \mathbf{E}\{|\tilde{x}_{kl}|^2\} &= |H_{kl,kl}|^2 + \sum_{(mn)\in\mathcal{I}\setminus(kl)} |H_{kl,mn}|^2 \\ &\leq |\underbrace{H_{kl,kl}}_{s}|^2 + \underbrace{B\|g\|^2 - |H_{kl,kl}|^2}_{\text{max. } I_{ext}} \end{aligned} \tag{13}$$

For an incomplete system $\boldsymbol{\mathcal{H}}^*$ possibly transforms g_{kl} into the $\mathcal{N}(\boldsymbol{\Gamma}\boldsymbol{\Gamma}^*)$ and $\mathbf{E}\{|\tilde{x}_{kl}|^2\}$ could tend to zero. Beside that $\boldsymbol{\Gamma}\boldsymbol{\Gamma}^*$ could commute with $\boldsymbol{\mathcal{H}}$ there is no more an overall energy conservation and in general

$$I_{ext} \leq B\|g\|^2 - |s|^2 \tag{14}$$

with equality for tight frames. In the same way the mean squared reconstruction error MSE in the carrier (kl) could be upper bounded to

$$\text{MSE} = \mathbf{E}\{|\tilde{x}_{kl} - x_{kl}|^2\} \leq B\|g\|^2 + 1 - 2 \cdot \text{Re}\{s\} \tag{15}$$

[4]We do not write here the (kl)-dependence. See Sec.II-C

with equality again for tight frames. For the "*signal to interference and noise ratio*" SINR follows that

$$\text{SINR} = \frac{|s|^2}{\sigma_{\tilde{n}}^2 + I_{ext}} \geq \frac{|s|^2}{\sigma_{\tilde{n}}^2 + B\|g\|^2 - |s|^2} \tag{16}$$

Note here that maximizing $|s|^2$ is minimizing I_{ext} is maximizing the SINR.

C. The cross ambiguity function

As long as the action of channel consist only of time shifts and modulations of the input signal the coupling is given by the cross ambiguity functions $\mathbf{A}_{g\gamma}(\cdot,\cdot)$

$$\mathbf{A}_{g\gamma}(\tau,\nu) = g^* \mathcal{M}_\nu \mathcal{T}_\tau \gamma \tag{17}$$

The coupling $H_{kl,mn}$ of carrier (kl) with carrier (mn) for a time shift $\mathcal{T}_\tau$ and a modulation $\mathcal{M}_\nu$ is

$$\begin{aligned} (\boldsymbol{G}^* \mathcal{M}_\nu \mathcal{T}_\tau \boldsymbol{\Gamma})_{kl,mn} &= \mathbf{A}_{g\gamma}((n-l)T + \tau, (m-k)F + \nu) \\ &\times e^{i2\pi[(m-k)lTF + \nu lT + \tau mF]} \end{aligned} \tag{18}$$

Because of linearity in these equations its easy extent this to weighted contributions like the *delay-Doppler spreading function* $h(\tau,\nu)$. Following Sec.II-B on Equ.(18) yields

$$\begin{aligned} s &= e^{i2\pi(\nu lT + \tau mF)} \mathbf{A}_{g\gamma}(\tau,\nu) \\ \text{MSE} &\leq B\|g\|^2 + 1 - 2\cos 2\pi(\nu lT + \tau kF) \cdot \text{Re}\{\mathbf{A}_{g\gamma}(\tau,\nu)\}) \\ I_{ext} &\leq B\|g\|^2 - |\mathbf{A}_{g\gamma}(\tau,\nu)|^2 \\ \text{SINR} &\geq \frac{|\mathbf{A}_{g\gamma}(\tau,\nu)|^2}{\sigma_{\tilde{n}}^2 + B\|g\|^2 - |\mathbf{A}_{g\gamma}(\tau,\nu)|^2} \end{aligned} \tag{19}$$

where $|s|^2$, I_{ext} and the SINR are independent of (kl) but the MSE could still be affected by symbol rotations depending on (kl). For rectangular pulses γ and g of width Π the cross ambiguity function is $\mathbf{A}_{g\gamma}(\tau,\nu) = \frac{\sin \pi\nu(\Pi-\tau)}{\pi\Pi\nu} e^{-i\pi\nu|\tau|}$ for $\tau \in (-\Pi, \Pi)$ and vanishes outside.

D. Frequency offset

As a simple application of the Sec.II-B and II-C considering now distortions caused by a constant unknown frequency offset. Let the receiver be able to estimate a phase error within some period. The self coupling s in the presence of a constant tone $\boldsymbol{\mathcal{H}} = e^{i(2\pi\omega t + \phi_0)}$ following section Sec.II-C is

$$s = e^{i(2\pi\omega lT + \phi_0)} \mathbf{A}_{g\gamma}(0,\omega) \tag{20}$$

For $\phi_0 = 0$ the phase is zero in the middle of the pulse because the pulse is centered around $t = 0$. Obviously this minimizes the MSE within a time slot. But its often convient to set the phase to zero at the beginning of the time slot at $-T/2$, hence $\phi_0 = -\pi\omega T$. We continue at first with the latter case to make comparisons to other authors

$$s = e^{-i\pi\omega T} e^{i2\pi\omega lT} \mathbf{A}_{g\gamma}(0, \omega) \tag{21}$$

To derive the MSE and I_{ext} for conventional OFDM consider rectangular pulses in $\mathbf{A}_{g\gamma}(\cdot,\cdot)$ of length $\Pi = T - T_{cp}$ sampled at M point (M is the number of carriers). For a duration of the modulation of only one OFDM–symbol length T we can set $l = 0$. We will neglect $\phi_0 \longrightarrow \phi_0 + \pi\omega\frac{1}{2M}$ accumulated within a sample. With $\nu = \omega/F = \omega\Pi$ in terms of the carrier separation F follows

$$\begin{aligned} s &= e^{-i\pi\nu} \frac{\sin \pi\nu}{\pi\nu} \\ I_{all} = \text{MSE} &= 2 - \frac{\sin 2\pi\nu}{\pi\nu} \\ I_{ext} &= 1 - \frac{\sin^2 \pi\nu}{(\pi\nu)^2} \end{aligned} \tag{22}$$

The formula for I_{ext} agrees with the result from [9]. They found for $\nu \leq .5$ a lower bound for the SINR (see Equ.(16) and)

$$\text{SINR} = \frac{\sigma_{\tilde{n}}^{-2} |s|^2}{1 + I_{ext} \cdot \sigma_{\tilde{n}}^{-2}} \geq \frac{\sigma_{\tilde{n}}^{-2} |s|^2}{1 + 0,5947 \cdot \sigma_{\tilde{n}}^{-2} \sin^2 \pi\nu} \tag{23}$$

where their numerically estimated bound for the interference is exact $I_{ext} \leq 0,5947 = 1 - \frac{4}{\pi^2}$ (Equ.(22)).

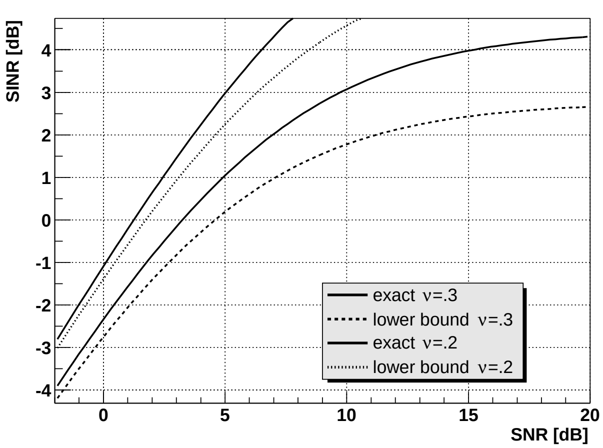

Fig. 1. *SINR vs. SNR in the presence of a constant frequency offset* – For comparison the resulting exact SINR (see Equ.(22)) and the lower bound (see Equ.(23)) in an OFDM system are shown versus the $\text{SNR} = \sigma_{\tilde{n}}^{-2}$ without the frequency offset.

III. Performance Comparison

A. Pulse shaping

In BFDM and NOFDM system design the time–frequency–carriers are not uncorrelated. The procedure of decorrelation $\gamma \longrightarrow \tilde{\gamma}$ (in the literature known as the "$S^{-1/2}$-trick")

$$\tilde{\gamma} = (\mathbf{\Gamma}\mathbf{\Gamma}^*)^{-1/2} \gamma \tag{24}$$

arranges the pulses in a constellation where for a single carrier the sum coupling to all other carriers is independent of the carrier. The set $\tilde{\gamma}_{mn} = \mathcal{M}_{mF} \mathcal{T}_{nT} \tilde{\gamma}$ forms a tight frame if the $\{\gamma_{mn}\}$ form a frame, hence $\tilde{\mathbf{\Gamma}}\tilde{\mathbf{\Gamma}}^* = \tilde{B} \cdot \mathbb{I}_{\mathcal{B}}$ and $\tilde{g} = \tilde{\gamma}$. That is using

$$\begin{aligned} 0 \leq \sum_{(mn) \neq (kl)} |\tilde{\gamma}_{mn}^* \tilde{\gamma}_{kl}|^2 &= \tilde{\gamma}_{kl}^* \tilde{\mathbf{\Gamma}}\tilde{\mathbf{\Gamma}}^* \tilde{\gamma}_{kl} - \|\tilde{\gamma}_{kl}\|^4 \\ &= (\tilde{B} - \|\tilde{\gamma}_{kl}\|^2) \|\tilde{\gamma}_{kl}\|^2 = (1 - TF)TF \end{aligned} \tag{25}$$

where the last step is only for Gabor frames in our normalization ($\tilde{B} = 1$). In the case of linear independency (in BFDM) the new pulses $\{\tilde{\gamma}_{mn}\}$ are completly decorrelated, hence they are orthogonal[5] and the setup is a *pulse shaped OFDM* system (to avoid confusion we still call it pulse shaped BFDM). In the proposed NOFDM scheme the correlation can not be canceled out completly due to missing dimensions but is uniform distributed over the subcarriers – the pulse set forms a tight frame.

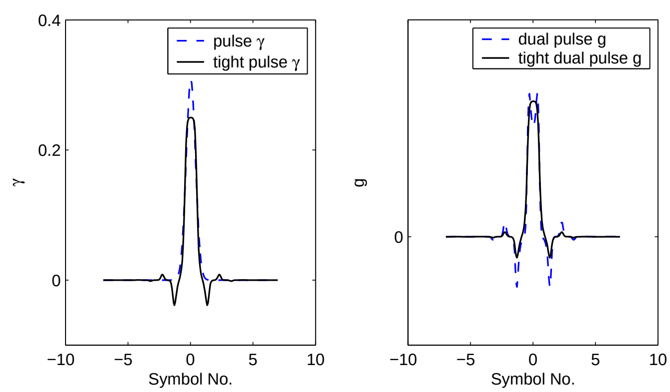

Fig. 2. *tight transmitter and receiver pulses* - an example for square lattice NOFDM using gaussians as input to the pulse shaping with $TF = 0.875$, hence $\epsilon \approx 1.14$.

B. Interference due to a frequency offset

To make a realistic comparison between the various MC approaches with different ϵ's we have fixed the outer data rate. The transmit signal undergoes modulations of a fixed

[5] Therefore this procedure is sometimes called orthogonalization. But in contrast to Gram-Schmidt it preserves properties of γ in that way that $\|\tilde{\gamma} - \gamma\|^2$ gets minimized.

duration equal to the OFDM symbol length for $\epsilon = 1$. After this time the receiver should be able to reconstruct the phase and correct for it optimally, hence set the phase to zero in the pulse center. Additionally we investigated cp–OFDM and the proposed pulse shaped BFDM on a rectangular lattice, both with $\epsilon \approx 0.57$. The input to the proposed pulse shaping scheme were gaussians $\sim e^{-\alpha\pi t^2}$ with $\alpha \approx F/T \approx 3$. As the counterpart to OFDM – we examined square-lattice NOFDM with $\epsilon = 1.14$. The input to the pulse optimization were again gaussians with $\alpha \approx F/T \approx 1$. With the shorter pulse cp–OFDM is more resistent to the frequency offset due to its increased carrier separation. In addition its only affected by an ϵ-portion of the complete modulation. In contrast the pulse shaped BFDM uses the redundancy – it is affected by the complete modulation. The theoretical MSE of Sec.II-D do well agree with the simulation except for the incomplete pulse shaped OFDM where it can only be an upper bound (see Fig.3). The iterative receiver in NOFDM removes the remaining interference as long the frequency offset is not too large.

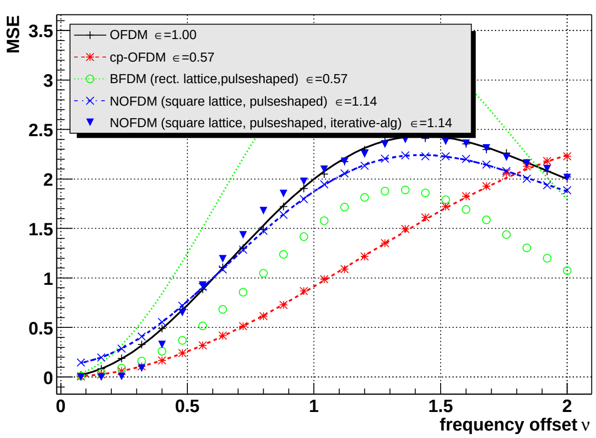

Fig. 3. *MSE comparison for different MC models* - the reconstruction error per channel is shown versus the normalized frequency offset. The frequency offset is normalized to the carrier separation of "$\epsilon = 1$"–OFDM. In addition the theoretical curves/bounds of Sec.II-D are included.

C. *Symbol error rates*

A frequency offset has significant impact on the symbol error rates. Obviously the statistics of the interference has to be studied to make exact statements. However, to give a sample Fig.4 shows the symbol error rate for BPSK at $\nu = 0.2$. cp–OFDM in contrast to pulse shaped BFDM mainly suffer from its loss in SNR. Pulse shaped NOFDM with its higher ϵ is able to follow the OFDM performance up to 18dB.

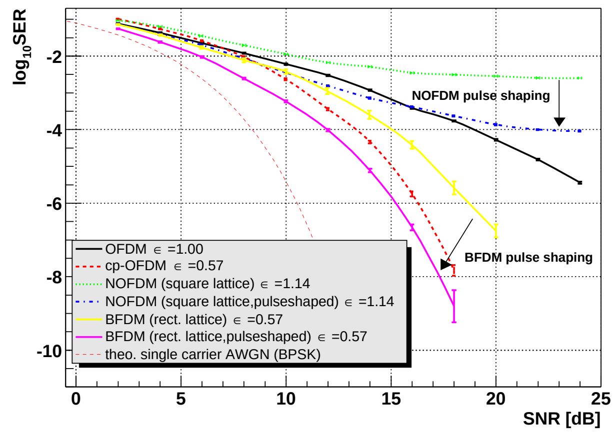

Fig. 4. *BPSK symbol error rate* - the impact of a frequency offset $\nu = 0.2$ on the BPSK performance is shown. Pulse shaped BFDM and cp–OFDM differ by the SNR loss of cp–OFDM. Up to 18dB pulse shaped NOFDM operates more bandefficient then OFDM. The pulse shaping significantly improves the error rates for BFDM/NOFDM.

IV. Conclusions

We studied various MC techniques under a frequency offset. We derived a common description of the interference term I_{ext} and the reconstruction error MSE which is verified by simulations. Finally we demonstrated the performance gain due to pulse shaping.

References

[1] Thomas Strohmer Hans G. Feichtinger, *Gabor Analysis and Algorithms - Theory and Applications*, Birkhäuser, 1998.

[2] Werner Kozek, "Nonorthogonal Pulseshapes for Multicarrier Communications in Doubly Dispersive Channels," *IEEE Journal on Selected Areas in Communications*, vol. 16, no. 8, pp. 1579–1589, Oct 1998.

[3] J. Ungermann W. Kozek, G. Pfander and G. Zimmermann, "A Comparison of Various MCM Schemes," *5th International OFDM-Workshop*, vol. 16, 2000.

[4] Th.Hunziker and D. Dahlhaus, "Iterative Symbol Detection for Bandwidth Efficient Nonorthogonal Multicarrier Transmission," *Trans. on Communications*, to appear 2002.

[5] I. Daubechies and A.J.E.M. Janssen, "Two theorems on lattice expansions," *IEEE Trans. Info. Theory*, vol. 39, no. 1, pp. 3–6, 1993.

[6] Th.Hunziker and D. Dahlhaus, "Iterative Symbol Detection for Bandwidth Efficient Nonorthogonal Multicarrier Transmission," *Proc. IEEE Vehicular Technology Conference (VTC 2000 Spring)*, vol. 1, pp. 61–65, 2000.

[7] A.J.E.M. Janssen, "From continuous to discrete Weyl–Heisenberg frames through sampling," *J. Fourier. Anal. Appl.*, vol. 3(5), pp. 583:596, 1997.

[8] Thomas Strohmer, "Rates of convergence for the approximation of dual shift–invariant system in $l^2(\mathcal{Z})$," *to appear in J. Fourier. Anal. Appl.*

[9] Paul H. Moose, "A Technique for Orthogonal Frequency Division Multiplexing Frequency Offset Correction," *Trans. on Communications*, vol. 42, no. 10, Oct 1994.